

## Hydrodynamic limit for the spin dynamics of the Heisenberg chain from quantum Monte Carlo calculations

Simon Grossjohann\* and Wolfram Brenig

*Institut für Theoretische Physik, Technische Universität Braunschweig, 38106 Braunschweig, Germany*

(Received 23 September 2009; published 20 January 2010)

We show that quantum Monte Carlo calculations of the dynamic structure factor of the isotropic-spin-1/2 antiferromagnetic chain at intermediate temperatures corroborate a picture of diffusive spin dynamics at finite frequencies in the low-energy long-wavelength limit and are in good agreement with recent predictions for this by Sirker *et al.* [Phys. Rev. Lett. **103**, 216602 (2009)].

DOI: [10.1103/PhysRevB.81.012404](https://doi.org/10.1103/PhysRevB.81.012404)

PACS number(s): 72.10.-d, 05.60.Gg, 05.10.Ln, 75.40.Gb

The one-dimensional (1D) Heisenberg XXZ antiferromagnet

$$H = J \sum_l \left[ \Delta S_l^z S_{l+1}^z + \frac{1}{2} (S_l^+ S_{l+1}^- + S_l^- S_{l+1}^+) \right], \quad (1)$$

where  $J > 0$  is the exchange coupling,  $S_l^{\pm}$  are spin-1/2 operators on site  $l$ , and  $\Delta$  is the exchange anisotropy which is one of the best studied strongly correlated many-body system. Its magnetic transport properties however, remain an open issue.<sup>1</sup> Spin transport in the Heisenberg chain is directly related to carrier transport in 1D correlated spinless fermion systems, via the Jordan-Wigner transformation, and therefore is of great interest in a broader context. Linear-response theory<sup>2</sup> shows the zero momentum, frequency-dependent spin conductivity

$$\sigma'(\omega) = D \delta(\omega) + \sigma'_{reg}(\omega) \quad (2)$$

to consist of the Drude weight

$$D = \frac{\beta}{N} \sum_{\substack{m,n \\ E_m = E_n}} e^{-\beta E_m} |\langle m | j | n \rangle|^2 \quad (3)$$

and a regular spectrum

$$\sigma'_{reg}(\omega) = \frac{1 - e^{-\beta\omega}}{\omega} \frac{1}{N} \sum_{\substack{m,n \\ E_m \neq E_n}} [e^{-\beta E_m} \times |\langle m | j | n \rangle|^2 \delta(\omega - E_n + E_m)], \quad (4)$$

where  $j = j_{q=0}$  is the  $z$  component of the spin current with  $j_q = (i\Delta J/2) \sum_l \exp(-iql) (S_l^- S_{l+1}^+ - S_l^+ S_{l+1}^-)$ , and  $m$  and  $n$  are the eigenstates with energies  $E_{m,n}$ .

The Drude weight has been under intense scrutiny for more than two decades. However, no generally accepted picture has emerged. A nonzero Drude weight would imply dissipationless transport in a correlated system,<sup>3</sup> despite the fact that  $[j, H] \neq 0$  for the XXZ model. Here we give a brief summary regarding the status of this issue and refer to Ref. 1, and references therein for a more extensive summary. At  $T = 0$  and in the massless regime  $|\Delta| < 1$  of the XXZ chain, the zero-temperature Drude weight is known to be finite.<sup>4</sup> At  $T \neq 0$ , Bethe-Ansatz (BA) calculations arrive at contradictory results regarding the temperature dependence of  $D(T)$ .<sup>5-7</sup>

The same holds for the question whether  $D(T > 0)$  is finite or not at the SU(2) symmetric point  $\Delta = 1$ .<sup>5,6</sup> Recent numerical studies using quantum Monte Carlo (QMC),<sup>8,9</sup> exact diagonalization (ED) at zero,<sup>2,10-12</sup> as well as finite magnetic fields,<sup>13</sup> and master equations<sup>14,15</sup> are consistent with  $D \neq 0$  for  $|\Delta| \leq 1$  and  $T \geq 0$ , supporting a ballistic contribution to the conductivity at finite temperatures. Recent time-dependent density-matrix renormalization-group studies have given evidence for ballistic spin dynamics for  $|\Delta| \leq 1$  in the out-of-equilibrium case.<sup>16</sup>

The regular finite-frequency contribution  $\sigma'_{reg}(\omega)$  has been considered by ED studies,<sup>17,18</sup> which however leave many open issues. Very recently, spin diffusion has been conjectured to govern the low-frequency spectrum of the regular conductivity,<sup>20</sup> based on real-time transfer-matrix renormalization group (tTMRG) and a perturbative analysis using bosonization. The latter provides for an approximate expression for the Fourier transform of the retarded spin susceptibility  $\chi_{ret}(q, t) = i\Theta(t) \langle [S_q^z(t), S_{-q}^z] \rangle$ , which reads

$$\chi_{ret}(q, \omega) = - \frac{Kvq^2}{2\pi} \frac{1}{\omega^2 - v^2q^2 - \Pi_{ret}(q, \omega)} \quad (5)$$

with

$$\Pi_{ret}(q, \omega) \approx -2i\gamma_B\omega - b\omega^2 + cv^2q^2, \quad (6)$$

where at  $\Delta = 1$ ,  $K = 1 + g/2 + g^2/4 + g^3/8$ ,  $v = \pi/2$  (see, e.g., Ref. 19),  $2\gamma_B = \pi g^2 T$ ,  $b = g^2/4 - g^3(3 - 8\pi^2/3)/32 + \sqrt{3}T^2/\pi$ , and  $c = g^2/4 - 3g^3/32 - \sqrt{3}T^2/\pi$  have been obtained by perturbative expansions (PEs) at  $T \ll J$  (Ref. 20) in powers of the running coupling constant  $1/g + \ln(g)/2 = \ln[\sqrt{\pi/2} \exp(G + 1/4)/T]$  and  $G \approx 0.577216 \dots$  is Euler's constant.<sup>21</sup>

Some remarks are in order. First, for  $\omega \ll \gamma$ , Eq. (5) displays a diffusion pole with a diffusion constant  $\Gamma = (1+c)v^2/(\pi g^2 T)$ . That is, within this approximation the spin dynamics of the Heisenberg chain would allow for a plain hydrodynamic limit. Second, Eqs. (5) and (6) do not incorporate the finite width of the spectral function  $\chi''(q, \omega) = \text{Im}[\chi_{ret}(q, \omega)]/\pi$  at  $T = 0$ , which is dominantly set by the two-spinon continuum. However, at  $q/\pi \ll 1$  the latter width is of order  $\pi J q^3/16$ , which for those wave vectors and temperatures which we will be interested in is negligible against  $\gamma_B$ . Third, for any finite momentum  $q \neq 0$ , the isothermal susceptibility  $\chi_q = \int_{-\infty}^{\infty} d\omega \chi''(q, \omega)/\omega$  obtained from Eq. (5) is identical to the isolated susceptibility  $\chi_{ret}(q, 0)$

$= \int_{-\infty}^{\infty} d\omega \chi''(q, \omega) / (\omega - i0^+)$  since  $\chi''(q \neq 0, \omega \rightarrow 0) \propto \omega$ . Therefore  $\chi_q = K / [2\pi v(1+c)]$ . Furthermore, the isothermal susceptibility of the Heisenberg model is a continuous function of  $q$ . Its limiting value  $\lim_{q \rightarrow 0} \chi_q = \chi_0$  at zero momentum is known from thermodynamic BA (TBA).<sup>19,21</sup> Therefore

$$\frac{K/(2\pi)}{v(1+c)} = \chi_0 \approx \frac{1}{\pi^2} \left( 1 - \frac{g}{2} + \frac{3g^3}{32} + \frac{\sqrt{3}T^2}{\pi} \right) = \chi_{PE} \quad (7)$$

should be satisfied, where  $\chi_{PE}$  is a known PE of the TBA result<sup>19,21</sup> and which is consistent with the parameters listed following Eq. (6).

The spectral function  $\chi''(q, \omega)$  is related to  $\sigma'_{reg}(\omega)$  by means of the lattice version of the continuity equation  $\partial_t S_q^z = [1 - \exp(-iq)]j_q$  through

$$\sigma'_{reg}(\omega) = \lim_{q \rightarrow 0} \frac{\omega}{q^2} \chi''(q, \omega). \quad (8)$$

Therefore, the spectrum of the regular part of the optical conductivity can be deduced from Eqs. (5) and (6).

The main goal of this work is to analyze, to which extent Eqs. (5) and (6) are consistent with QMC calculations. The significance of such comparison is with the regular part of the spin conductivity. It will *not* clarify the size of the Drude weight, as any discrepancy arising may be due to partial spectral weight transfer into a Drude weight. Furthermore, we focus on the isotropic point  $\Delta=1$ , which may be different from the anisotropic case. To begin, we note, that Eqs. (5) and (6) approximate the on-shell part of the spectrum for  $|\omega \pm vq| \ll T$ . Yet, similar to the comparison with tTMRG in Eqs. (C2) and (C3) of Ref. 20, we will assume them to be valid for all  $\omega$ . Furthermore,  $\chi_q$  is known to monotonously increase for the Heisenberg model as  $q \rightarrow \pi/2$ . However,  $\chi_q = K/[2\pi v(1+c)]$  from bosonization is momentum independent. Therefore, a momentum dependence  $K \rightarrow K_q$  and  $v \rightarrow v_q$ —albeit weak at  $q \ll 1$ —is to be allowed for, when matching up Eqs. (5) and (6) with QMC.

We perform the comparison to QMC by transforming  $\chi_{rel}(q, \omega)$  onto the imaginary-time axis

$$\chi(q, \tau) = 2 \sum_{n=0}^{\infty} \cos(\omega_n \tau) \chi(q, \omega_n) - \chi(q, 0),$$

$$\chi(q, \omega_n) = \frac{K_q v_q q^2 / (2\pi)}{(1+b)\omega_n^2 + (1+c)v_q^2 q^2 + 2\gamma_q |\omega_n|}. \quad (9)$$

The main point is that a corresponding  $\chi_{QMC}(q, \tau)$  can be obtained directly from QMC, following preceding work employing the stochastic series-expansion method.<sup>22</sup> This involves only the statistical error, which is well controlled. Uncontrolled sources of error, due to, e.g., transformations to real or Matsubara frequencies, do not occur.  $\chi(q, \tau)$  is gauged against  $\chi_{QMC}(q, \tau)$  by fitting  $K_q$ ,  $v_q$ , and  $\gamma_q$  at *small* momentum while retaining  $b$  and  $c$  as given by bosonization. This is justified because the latter two constants do not enlarge the space of fitting parameter, as any modification of them can be absorbed into a renormalization of  $K_q$ ,  $v_q$ , and  $\gamma_q$ . Regarding the temperature range, we confine ourselves to  $T/J \leq 0.25$ . This is motivated by the PE to  $O(g^3, T^2)$  for ther-

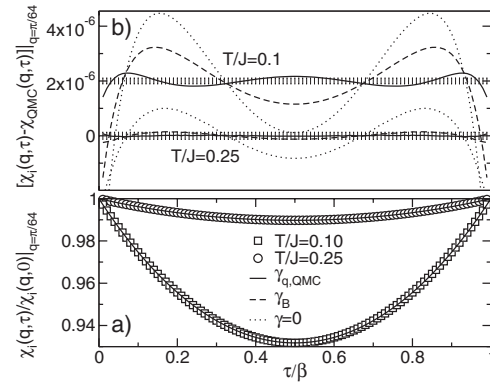


FIG. 1. Imaginary-time susceptibility  $\chi_{QMC}(q, \tau)$  at  $q = \pi/64$  on 128 sites, for two temperatures  $T$ , fitted to  $\chi(q, \tau)$  from Eq. (9) (lines) in three ways, namely,  $\gamma_{q,QMC}$  optimized (solid),  $\gamma_B$  taken from Ref. 20 (dashed), and  $\gamma$  forced to zero (dotted). The index “ $i$ ” on the y axis refers to  $\chi(q, \tau)$  from Eq. (9) for the lines in panels (a) and (b) as well as to QMC for the symbols in panel (a). Panel (a) Global behavior of  $\chi_{QMC}(q, \tau)/\chi_{QMC}(q, 0)$  for  $T/J=0.1$  (QMC, squares) and 0.25 (QMC, circles). In this panel the three fits (lines) are indistinguishable on the scale of the plot. Panel (b) error  $2\sigma$  of  $\chi_{QMC}(q, \tau)$  for each  $\tau$  evaluated (error bars) and difference  $\chi(q, \tau) - \chi_{QMC}(q, \tau)$  between QMC and the three fits (lines).  $2\sigma$  for the QMC data is  $O(10^{-7})$ . Plots corresponding to  $T/J=0.1$  have been shifted by  $2 \times 10^{-6}$ .

modynamic properties to agree rather well with QMC results up to  $T/J \leq 0.1$  (Ref. 23) while for  $T \geq 0.25$  the PE starts to fail significantly.

Figure 1 shows the result of the comparison of QMC with Eq. (9) for the smallest nonzero wave vector  $q = \pi/64$  of a 128-site system for two temperatures  $T/J=0.1$  and 0.25 allowing for three different choices of  $\gamma_q$ , namely, (i)  $\gamma_{q,QMC}$  as optimized by fitting, (ii)  $\gamma_B$  taken from the bosonization, and finally (iii)  $\gamma_q=0$  forced to be zero.<sup>24</sup> The upper panel (b) of this figure clearly demonstrates that QMC is inconsistent with  $\gamma_q=0$  and that increasing  $\gamma_q$  above zero improves the quality of the fit. In particular, the best fit, i.e., for  $\gamma_{q,QMC}$ , is identical within the standard deviation  $2\sigma$  (error bar) to QMC for almost all  $\tau \in [0, \beta]$  at both temperatures. Yet, we find  $\gamma_{q,QMC} > \gamma_B$  and moreover there are *systematic* oscillatory deviations. While the latter seem a subdominant effect, which could be due to the on-shell approximation in Eqs. (5) and (6), these deviations may also indicate relevant corrections to diffusion and should be investigated in future studies. We emphasize the vertical scale on panel (b) of Fig. 1 which demonstrates that high-precision QMC is mandatory for the present analysis. Figure 1 is a central result of this work. It shows that QMC is consistent with a dynamic structure factor of the isotropic antiferromagnetic Heisenberg chain which is approximately diffusive at intermediate temperatures in the long-wavelength limit with a diffusion kernel  $(1+c)v^2/(2\gamma_{q,QMC})$ . Any momentum dependence of  $\gamma_{q,QMC}$  to be discussed later, implies corrections to this diffusion. Next, and to further support our approach, we will also discuss the Luttinger parameters we find.

In Table I we compare the parameters obtained from the fit to QMC with results from TBA, PE, and tTMRG. This

TABLE I. Columns 2 and 3: comparison of  $\chi_{q,\text{QMC}}=K_q/[2\pi v_q(1+c)]$  from QMC at  $q=\pi/64$  with  $\chi_0$  from TBA (Ref. 25) and  $\chi_{\text{PE}}$  from the lhs of Eq. (7). Columns 4–6 display  $\gamma$  from bosonization, tTMRG, and QMC.

$T/J$	$\chi_{q,\text{QMC}}/\chi_0$	$\chi_{q,\text{QMC}}/\chi_{\text{PE}}$	$\gamma_B$ (Ref. 20)	$\gamma_{\text{TMRG}}$ (Ref. 20)	$\gamma_{q,\text{QMC}}$
0.1	1.0005	1.0032	0.0096		0.0191
0.25	1.0005	1.0248	0.0440		0.0511
0.2			0.0297	0.0190	

table shows that  $\chi_{q,\text{QMC}}=K_q/[2\pi v_q(1+c)]$  at  $q=\pi/64$  is in excellent agreement with the isothermal susceptibility at  $q=0$  from the TBA for *both* temperatures which we have studied. This result should not be confused with the well-known agreement between static QMC and TBA for the isothermal susceptibility<sup>23</sup> but rather it is a satisfying consistency check for our approach. In fact, fitting the imaginary-time transform of an *approximate*  $\chi(q, \omega)$ , i.e., Eq. (5), to QMC could require values for  $K_q$ ,  $v_q$ , and  $\gamma_q$  which deviate from exactly known values for these quantities on a scale which is unrelated to the error  $2\sigma$  of the QMC. As will be shown later the variation in  $K_q$  and  $v_q$  with momentum is very weak as  $q \ll 1$ , i.e., we expect no relevant change for  $\chi_{q,\text{QMC}}$  as  $q \rightarrow 0$ . Yet we are tempted to point out that  $\chi_{q=\pi/64,\text{QMC}}$  in Table I is barely larger than  $\chi_0$ , which is consistent with the momentum dependence for the exact  $\chi_q$ . The fact that  $\chi_{q,\text{QMC}}/\chi_{\text{PE}} > 1$  and is increasing as  $T$  increases, evidences that  $\chi_{\text{PE}}$  on the left-hand side (lhs) of Eq. (7) increasingly underestimates the TBA result as  $T$  increases beyond  $T/J \gtrsim 0.1$ . In Fig. 1 we have shown that  $\gamma_{q,\text{QMC}} \neq \gamma_B$ . Yet, Table I demonstrates that  $\gamma_{q,\text{QMC}}$  and  $\gamma_B$  are comparable to within factors of order 2. Most important, the relaxation rate  $\gamma_{q,\text{QMC}}$  we find is much larger than the width of the two-spinon continuum, yet, very small compared to temperature  $\gamma_{q,\text{QMC}} \ll T$ . We note that fits to tTMRG (Ref. 20) at  $T/J=0.2$  lead to  $\gamma_{\text{TMRG}}/\gamma_B \approx 0.64$ .

Next we discuss the momentum dependence. Figure 2 displays all three fit parameters  $K_q$ ,  $v_q$ , and  $\gamma_{q,\text{QMC}}$  versus the first six nonzero momenta and the two temperatures  $T/J=0.1$  and  $0.25$  which have also been considered in Fig. 2.  $v_q$  and  $\gamma_{q,\text{QMC}}$  have been normalized to their values given by

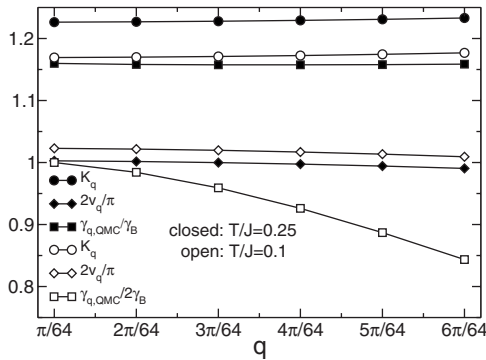


FIG. 2. Momentum dependence of the renormalized Luttinger parameter  $K_q$ , spinon velocity  $v_q$ , and scattering rate  $\gamma_{q,\text{QMC}}/\gamma_B$  for the first nonzero six momenta on a 128 site system for two temperatures  $T/J=0.1$  (white symbols) and  $0.25$  (black symbols). Note that  $\gamma_{q,\text{QMC}}/\gamma_B$  for  $T=0.1$  has been scaled by 2 to fit into the plot.

bosonization, i.e.,  $\pi/2$  and  $\gamma_B$ . Obviously all momentum variations are very smooth and rather weak. As can be seen from this figure, most of the renormalization of the ratio  $K_q/v_q$  from its bare value of  $2/\pi$  stems from  $K_q > 1$ . The spinon velocity  $v_q$  deviates slightly from  $\pi/2$ , however, only to within  $O(1\%)$ . As discussed in the previous paragraph, this is necessary to obtain an optimum fit of the QMC to the approximation Eq. (9) and does *not* imply that QMC is at variance with the bare spinon velocity.  $K_q$  displays a very weak upward curvature while  $v_q$  shows a small downward curvature. The latter can be understood in terms of  $O(q^3)$  corrections to the linear on-shell dispersion  $\omega(q)$  which are not contained in bosonization. The combined momentum dependence of  $K_q/v_q$  leads to the expected increase in the static susceptibility with  $q$ . Finally,  $\gamma_{q,\text{QMC}}/\gamma_B$  also displays a weak momentum dependence which is larger for  $T/J=0.1$ . The latter may signal the onset of finite-size effects. In fact,  $\gamma_{q,\text{QMC}} \neq 0$  implies a length scale  $l$  of order  $O[v/(2\gamma_{q,\text{QMC}})]$  for the regular current relaxation.  $l$  is less than the system size for both temperatures studied. Yet,  $128/l \approx 9$  for  $T/J=0.25$  and  $128/l \approx 3$  for  $T/J=0.1$ . With momentum dependence,  $\gamma$  as extracted from a real-space quantity<sup>20</sup> will differ from that obtained by QMC at fixed small momenta.

While the preceding has been exact up to the statistical error of the QMC, we would like to conclude this work by speculating on the line shape of the regular part of the conductivity on the imaginary frequency axis at  $\omega_n=2\pi nT$ . In principle this requires a careful analysis of the error introduced by the Fourier transform  $\chi_{\text{QMC}}(q, \omega_n) = \int_0^{1/T} \exp(i\omega_n\tau) \chi_{\text{QMC}}(q, \tau) d\tau$ . This error will increase as  $\omega_n$  increases. Here we refrain from analyzing this since our goal is merely to demonstrate to which extend our QMC data discriminates between a conductivity with  $\gamma=0$  and one with  $\gamma=\gamma_{q,\text{QMC}} \neq 0$ . To this end Fig. 3 displays  $\omega_n \sigma_{\text{QMC}}(q, \omega_n) = \omega_n^2 \chi_{\text{QMC}}(q, \omega_n)/q^2$  as compared to  $\omega_n \sigma(q, \omega_n) = \omega_n^2 \chi(q, \omega_n)/q^2$  with  $\chi(q, \omega_n)$  taken from Eq. (9) and with  $\gamma=0$  or  $\gamma=\gamma_{q,\text{QMC}}$ . Without any further ado, this figure clearly demonstrates that  $\gamma=0$  in  $\sigma(q, \omega_n)$  from Eqs. (8) and (9) is inconsistent with our QMC which however agrees very well with  $\sigma(q, \omega_n)$  for  $\gamma=\gamma_{q,\text{QMC}}$ .<sup>26</sup> This implies that QMC is consistent with a Drude type of behavior of the frequency dependence of the regular conductivity with a relaxation rate  $2\gamma_{q,\text{QMC}}$ . While future studies may focus on finite-size scaling to perform the limit of  $q \rightarrow 0$ , as required in Eq. (8), this is beyond the scope of the present analysis.

In conclusion QMC is consistent with spin dynamics of the isotropic 1D Heisenberg antiferromagnet which is primarily diffusive in the long-wavelength limit and at intermediate temperatures, implying a *regular* part of the spin conduc-

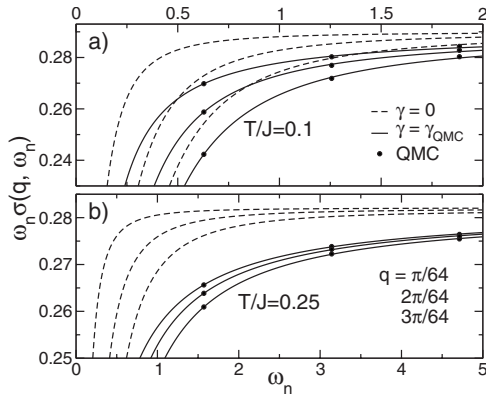


FIG. 3.  $\omega_n \sigma_{\text{QMC}}(q, \omega_n)$  from QMC for the first three nonzero Matsubara frequencies  $\omega_n = 2\pi nT$  and wave vectors  $q = n\pi/64$ , with  $n = 1, 2, 3$  as compared to  $\omega_n^2 \chi(q, \omega_n)/q^2$  using Eq. (9) with  $\gamma = 0$  (dashed) and  $\gamma = \gamma_{q, \text{QMC}}$  (solid) on a 128 site system for (a)  $T/J = 0.1$  and (b) 0.25. (See text regarding statistical error.)

tivity with a finite relaxation rate  $\gamma \ll T$ . This corroborates recent findings by bosonization and tTMRG. Our analysis does not allow conclusions on the pending open questions on the Drude weight at  $\Delta = 1$ , yet based on the numerical evidence for  $D(T > 0) > 0$ , our findings may open up the intriguing possibility of a finite temperature dynamical spin conductivity of the isotropic Heisenberg model which comprises of both, a finite Drude weight and a regular part with a very large mean-free path at low temperatures. Future analysis should focus on the relevance of corrections beyond the on-shell approximation, on the case  $\Delta < 1$ , and on higher temperatures  $T \gtrsim J$ .

We are indebted to F. Heidrich-Meisner and R. G. Pereira for valuable comments. Work supported in part by the Deutsche Forschungsgemeinschaft through Grant No. BR 1084/6-1, FOR912 and by the National Science Foundation under Grant No. PHY05-51164.

\*s-n.grossjohann@tu-bs.de

- <sup>1</sup>F. Heidrich-Meisner, A. Honecker, and W. Brenig, *Eur. Phys. J. Spec. Top.* **151**, 135 (2007).
- <sup>2</sup>F. Heidrich-Meisner, A. Honecker, D. C. Cabra, and W. Brenig, *Phys. Rev. B* **68**, 134436 (2003).
- <sup>3</sup>X. Zotos, F. Naef, and P. Prelovšek, *Phys. Rev. B* **55**, 11029 (1997).
- <sup>4</sup>B. S. Shastry and B. Sutherland, *Phys. Rev. Lett.* **65**, 243 (1990).
- <sup>5</sup>X. Zotos, *Phys. Rev. Lett.* **82**, 1764 (1999).
- <sup>6</sup>J. Benz, T. Fukui, A. Klümper, and C. Scheeren, *J. Phys. Soc. Jpn. Suppl.* **74**, 181 (2005).
- <sup>7</sup>Z. Qiu-Lan and G. Shi-Jian, *Chin. Phys. Lett.* **24**, 1354 (2007).
- <sup>8</sup>J. V. Alvarez and C. Gros, *Phys. Rev. B* **66**, 094403 (2002).
- <sup>9</sup>D. Heidarian and S. Sorella, *Phys. Rev. B* **75**, 241104(R) (2007).
- <sup>10</sup>B. N. Narozhny, A. J. Millis, and N. Andrei, *Phys. Rev. B* **58**, R2921 (1998).
- <sup>11</sup>P. Jung and A. Rosch, *Phys. Rev. B* **76**, 245108 (2007).
- <sup>12</sup>S. Mukerjee and B. S. Shastry, *Phys. Rev. B* **77**, 245131 (2008).
- <sup>13</sup>F. Heidrich-Meisner, A. Honecker, and W. Brenig, *Phys. Rev. B* **71**, 184415 (2005).
- <sup>14</sup>T. Prosen and M. Znidaric, *J. Stat. Mech.: Theory Exp.* (2009)

P02035.

- <sup>15</sup>M. Michel, O. Hess, H. Wichterich, and J. Gemmer, *Phys. Rev. B* **77**, 104303 (2008).
- <sup>16</sup>S. Langer, F. Heidrich-Meisner, J. Gemmer, I. P. McCulloch, and U. Schollwöck, *Phys. Rev. B* **79**, 214409 (2009).
- <sup>17</sup>X. Zotos and P. Prelovšek, *Phys. Rev. B* **53**, 983 (1996).
- <sup>18</sup>F. Naef and X. Zotos, *J. Phys.: Condens. Matter* **10**, L183 (1998).
- <sup>19</sup>A. Klümper and D. C. Johnston, *Phys. Rev. Lett.* **84**, 4701 (2000).
- <sup>20</sup>J. Sirker, R. G. Pereira, and I. Affleck, *Phys. Rev. Lett.* **103**, 216602 (2009), arXiv:0906.1978v1.
- <sup>21</sup>S. Lukyanov, *Nucl. Phys. B* **522**, 533 (1998).
- <sup>22</sup>S. Grossjohann and W. Brenig, *Phys. Rev. B* **79**, 094409 (2009).
- <sup>23</sup>D. C. Johnston, R. K. Kremer, M. Troyer, X. Wang, A. Klümper, S. L. Bud'ko, A. F. Panchula, and P. C. Canfield, *Phys. Rev. B* **61**, 9558 (2000).
- <sup>24</sup>Fits performed using Mathematica®.
- <sup>25</sup>A. Klümper (private communication).
- <sup>26</sup>For a different QMC approach, not suited to clarify the role of  $\gamma$  in  $\sigma(q, \omega_n)$  see Ref. 20.